

Binary collision theory for thermal and nonisothermal relaxation and reaction of polyatomic molecules

Peter Talkner ^a, Eli Pollak ^b, Alexander M. Berezhkovskii ^c

^a *General Energy Research, Paul Scherrer Institut, CH-5232 Villigen, Switzerland*

^b *Chemical Physics Department, Weizmann Institute of Science, 76100 Rehovot, Israel*

^c *Karpov Institute of Physical Chemistry, 10 Vorontsovo Pole Str., 103064 Moscow, Russia*

Abstract

Many unimolecular reactions are initiated by photoexcitation of a polyatomic molecule at room temperature from its S_0 ground state to an electronically excited S_1 state. This excitation will generally lead to a nonisothermal initial distribution of energy in the excited state. Collisions with a buffer gas at room temperature tend to reequilibrate the reacting molecule. The ensuing radiative and nonradiative decay will depend on the competition between the energy dependent unimolecular decay rate and the energy relaxation. In this paper we describe a Gaussian binary collision theory which includes all three aspects – radiative decay, nonradiative decay and relaxation. The Gaussian property is justified when the reacting species is large enough, i.e. it has a large enough number of degrees of freedom such that the equilibrium distribution of the molecule can be described by a Gaussian. Guided by experimental observation, we adapt a Gaussian transition probability, which is similar to Mel'nikov's, to describe the relaxation dynamics. An analytic solution for the Gaussian master equation is presented. We find that pressure induced decay which is faster than the initial decay rate is an experimental signature of an initial cold distribution of reactants. This signature was observed experimentally in the isomerization of trans-stilbene. Application to the decay dynamics of the trans-stilbene molecule shows that an initial temperature of 230 K for trans-stilbene in the excited S_1 state suffices for good agreement between the theoretical and experimental survival probability measured at a gas temperature of 300 K.

1. Introduction

Ten years ago, Balk and Fleming [1] measured the fluorescence decay rate of trans-stilbene as a function of the pressure of a methane buffer gas. The experiment consisted of the laser excitation of thermal (room temperature) trans-stilbene from the S_0 to the S_1 electronically excited state, at the ground S_0 vibrational state to ground S_1 vibrational state frequency ($\hbar \omega_{00}$). In the excited state, the molecule can undergo isomerization to a more stable gauche

state. The reaction, which is a radiationless transition, prevents the normal fluorescence to the ground state, so that the fluorescence decay becomes a measure for the unimolecular reaction rate. Balk and Fleming found the following interesting features: (a) The fluorescence decay at low pressure was at least biexponential. (b) The initial decay rate increased with increasing buffer gas pressure, becoming larger than the thermal rate.

The second result was especially surprising: One would expect that the buffer gas would increase the

initial decay rate at most up to the thermal rate, as the thermal rate is the approximate upper bound predicted by transition state theory. Balk and Fleming analyzed their results using a binary collision model [2], which included both the possibility of reaction and relaxation via a step ladder model [3,4]. They found, that such a model predicts the expected: Pressure does not increase the initial decay rate beyond the thermal rate, in contradiction to the experimental finding.

Gershinsky and Pollak [5,6] have recently proposed a resolution of this ‘paradox’. They noted that excitation of trans-stilbene at the ω_{00} frequency should cause a significant cooling of the excited state population when compared to the ground state. This cooling, substantially lowers the rate of isomerization relative to that expected at room temperature. The initial decay rate of the isolated molecule reflects this cooling, and is substantially slower than the thermal decay rate at room temperature. Collisions with a room temperature buffer gas will cause a heating of the excited state population and thus an increase in the reaction rate. This qualitative explanation also allowed a reconciliation between the measured gas phase rates which were over an order of magnitude lower than rates measured by Schroeder et al. [7], in the presence of unassociated liquids. In the liquid, the excited state stilbene population is rapidly thermalized and so one measures the true room temperature rate constant.

This innocuous interpretation, would seem at first glance to contradict the predictions of Kramers rate theory [8], especially in the low friction regime, where Professor Mel’nikov made a seminal contribution [9]. Kramers’ theory predicts that the decay rate of reactants will be monoexponential and that it will be *independent* of the preparation of reactants in the initial state. If Kramers’ theory were applicable, then the initial cooling of trans-stilbene in the excited state would be irrelevant to the experimental decay profile and its dependence on pressure. The independence on initial conditions which is inherent to Kramers theory comes from the assumption that the energy barrier to reaction (V) is much larger than the thermal energy ($k_B T$), which in Kramers’ one dimensional model is also the equilibrium energy of the reacting molecule. Since the energy of the reactants is much lower than the barrier height, and since

the reaction time is exponentially large, any initial state preparation may be disregarded, as the reactants will equilibrate before they react.

Stilbene is a polyatomic molecule with 72 degrees of freedom. The energy barrier to reaction V is substantially lower than the equilibrium thermal energy E_{th} . Therefore, the molecule may react before relaxing to thermal equilibrium and it is for this reason that the decay may depend on the initial preparation of the molecule. The dependence on initial conditions is then a function of the ratio of time scales of relaxation and reaction. If the energy relaxation is fast relative to reaction – as might be expected in a liquid, then the decay rate will be independent of the initial preparation. But in the gas phase, at low enough pressure, the collision time becomes longer than the reaction time and one will find a dependence on the initial preparation.

In an unassociated liquid, the energy relaxation process can be modelled using an energy diffusion equation. We have recently shown [10] how such a model may lead to nonexponential decay in the liquid, provided that the energy relaxation and reaction time scales are comparable. Such a model is though not applicable to the gas phase reaction, where one should use a binary collision model. This is the central topic of this paper. In Section 2, we formulate a binary collision model. In this model the population of the reacting species is governed by a master equation, which allows for both energy relaxation, reaction and radiative decay. A master equation description of the process is in itself not new. The tough question is how one chooses to model the energy relaxation and reaction probabilities. One could choose the idealized model of Ref. [2], here we suggest a different approach, which stresses the multidimensional nature of the reacting molecule.

Mel’nikov, in his solution of the Kramers problem, showed that the energy transfer probability kernel relevant to Kramers’ problem, is a Gaussian, and that the average energy loss is a constant for initial energies near the barrier energy. Measurements of energy transfer for polyatomic molecules in the gas phase have demonstrated that in a wider range of energies, very often, the average energy loss per collision is linearly proportional to the initial energy [11,12]. This suggests that Mel’nikov’s Gaussian probability kernel may be modified to

model the energy relaxation dynamics also in the gas phase. The ‘trouble’ with such a choice is that in the absence of reaction, the modified kernel would lead to a Gaussian equilibrium distribution, which is not identical to the Boltzman distribution.

It is here too, that the polyatomic nature of the reactants becomes crucial. For a polyatomic molecule, the Boltzman distribution is a product of the density of states at energy E and the Boltzman factor $e^{-E/k_B T}$. Because of the multidimensional nature of a polyatomic molecule, the density of states increases with energy, so that the true equilibrium distribution is a bell shaped function, which approaches a Gaussian as the number of degrees of freedom is increased.

The resulting Gaussian binary collision model for the energy relaxation dynamics in the absence of reaction is solved analytically in Section 3. This analytic solution is then used in Section 4 to solve for the survival probability in the presence of reaction. The energy dependent reaction probability is modelled using the RRK theory [13]. This solution is then applied in Section 5 to a number of examples in which reactants are prepared at initial temperatures that differ from the equilibrium gas temperature. We find that this model provides a good explanation for the decay rates observed by Balk and Fleming in the stilbene isomerization reaction. We conclude with a discussion of the limitations of the model and possible improvements and extensions.

2. The Gaussian binary collision model

We consider an electronically excited polyatomic molecule immersed in a gas of inert molecules which is in thermal equilibrium at a temperature T . Due to the excitation process, the vibrational states of the excited molecule are initially populated according to a thermal distribution with temperature T_0 which may differ from the temperature of the surrounding gas. Collisions between the excited molecule and gas molecules will alter this distribution and let it approach thermal equilibrium at the temperature T of the surrounding gas. At the same time, the excited molecule can undergo a radiative transition or a radiationless transition to a different conformation, with a rate $K(E)$ which depends at most on the

vibrational energy E of the excited molecule. It is our goal to determine the life-time of the excited molecule.

The equilibrium distribution $p_{\text{eq}}(E)$ is given by the density of states of the excited molecule $\Omega(E)$ and the Boltzmann-factor at the inverse bath-temperature β :

$$p_{\text{eq}}(E) = Z^{-1} \Omega(E) e^{-\beta E}, \quad (2.1)$$

where Z is the partition function:

$$Z = \int dE \Omega(E) e^{-\beta E}. \quad (2.2)$$

The density of states of a polyatomic molecule is in general not known analytically. An exception is if the polyatomic molecule can be described as a collection of N harmonic degrees of freedom. In this case, the classical density of states takes the form:

$$\Omega(E) = \Omega_0 E^{N-1}, \quad (2.3)$$

where Ω_0 is a constant, independent of the energy E . The density of states is an increasing function of the energy, while the Boltzman factor ($e^{-\beta E}$) decreases with energy. This means that the thermal equilibrium distribution is a bell-shaped function which for a sufficiently high number of degrees of freedom, may be approximated as a Gaussian:

$$p_{\text{eq}}(E) \approx \beta / \sqrt{2\pi(N-1)} \times \exp \left[-\frac{\beta^2}{2(N-1)} \left(E - \frac{N-1}{\beta} \right)^2 \right]. \quad (2.4)$$

As the number of degrees of freedom N increases, the Gaussian becomes narrower and the Gaussian approximation becomes increasingly more accurate.

In principle, the range of allowed energy values E is bounded from below at $E = 0$. If N is sufficiently large, the distribution is narrow enough to allow the range of allowed energies to go from $-\infty$ to ∞ since the probability distribution will anyway be negligible at the negative energies. This extension of the boundary, which also appears in Mel’nikov’s solution of the Kramers problem, allows for an analytic solution of the energy redistribution dynamics, as shown in the next section.

A comparison between the thermal RRK equilibrium distribution and its Gaussian approximation is

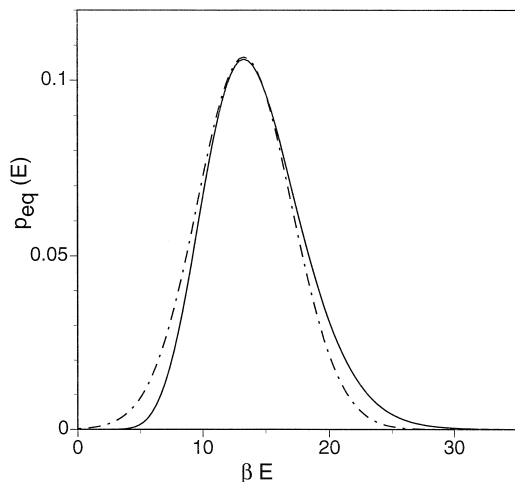


Fig. 1. Gaussian approximation for the canonical equilibrium distribution (cf. Eqs. (2.1) and (2.3)). The dashed dotted line is the Gaussian approximation for $N = 15$ (cf. Eq. (2.4)) the solid line is the exact distribution function. The abscissa is in reduced energy units (βE).

shown in Fig. 1 for a model with $N = 15$ degrees of freedom. Note that the quality of the fit does not depend on the temperature, as the temperature is scaled out of Eq. (2.4) by using the reduced energy variable βE . It only depends on the number of degrees of freedom N .

The next element in the construction of the binary collision model is the choice of the (normalised) transition probability kernel $p(E|E')$ which gives the conditional probability that a collision will change the energy of the reacting molecule from E' to E . Guided by Mel'nikov's solution to the Kramers equation in the underdamped limit, we will assume that the energy transfer is a Gaussian random process. At any collision, the energy transferred may be thus decomposed into an average energy transfer and a fluctuating energy transfer which has zero mean and is Gaussian distributed. Experimental observations [11,12] show that for polyatomic molecules, a good rule of thumb is that the average energy transferred per collision is linearly proportional to the energy prior to the collision. Specifically, the average transferred energy is assumed to be proportional to the difference between the initial energy E' and the average equilibrium energy at the temperature of the surrounding gas, which in the Gaussian limit is $E_{\text{th}} = (N - 1)/\beta$, cf. Eq. (2.4).

In principle, the fluctuational energy transfer should also be dependent on the initial energy of the excited molecule [12], however this dependence is not very strong. If the initial temperature of the excited molecule does not differ too strongly from that of the surrounding medium, then one may safely assume that the fluctuational term is also energy independent. These assumptions are summarised by the simple relation:

$$E - E' = -\alpha(E' - E_{\text{th}}) + \xi, \quad (2.5)$$

where α is the relative average transferred energy. The Gaussian distribution for the random energy transfer

$$\rho(\xi) = \frac{1}{\sqrt{2\pi\langle\xi^2\rangle}} e^{-\xi^2/(2\langle\xi^2\rangle)} \quad (2.6)$$

thus leads with Eq. (2.5) to the Gaussian transition probability

$$p(E|E') = \rho(E - E' + \alpha(E' - E_{\text{th}})). \quad (2.7)$$

For a gas in thermodynamic equilibrium, the transition probability kernel must satisfy the principle of detailed balance [15]:

$$p(E|E')p_{\text{eq}}(E') = p(E'|E)p_{\text{eq}}(E). \quad (2.8)$$

This imposes a relation between the strength (variance) of energy transfer fluctuations and the relative average energy transferred:

$$\langle\xi^2\rangle = \left[1 - (1 - \alpha)^2\right] \frac{N - 1}{\beta^2}, \quad 0 < \alpha < 2. \quad (2.9)$$

This means that the only free parameter in the probability kernel is the magnitude of the relative average energy transferred per collision α .

To complete the model, we must specify the energy dependent transition rate $K(E)$. We will assume that the radiationless unimolecular reaction rate is given by the RRK expression [13,14]:

$$k_{\text{RRK}}(E) = k_{\infty} \left(\frac{E - V}{E}\right)^{N-1} \theta(E - V). \quad (2.10)$$

It vanishes below the activation barrier energy $E = V$ and increases until it has reached an asymptotic value k_{∞} . It is of interest to estimate the magnitude

of the escape rate at the average thermal energy of the reactants $E_{\text{th}} = (N-1)k_{\text{B}}T$. For large enough N , one notes that:

$$k_{\text{RRK}}(E_{\text{th}}) = k_{\infty} \left[1 - \frac{V}{(N-1)k_{\text{B}}T} \right]^{N-1} \sim k_{\infty} e^{-V/k_{\text{B}}T} \ll 1. \quad (2.11)$$

This means, that even though the average thermal energy of the molecule is much larger than the barrier height, the reaction probability may still be exponentially small and well described by the Arrhenius factor. The total decay rate $K(E)$ will be a combination of the unimolecular reaction rate and an energy independent radiational transition rate.

We assume independent binary collisions between the buffer gas atoms (or molecules) and the reacting polyatomic molecule. This means that the waiting time between successive collisions is exponentially distributed [14,15]. The amount of energy transferred in such a collision is assumed to depend only on the internal vibrational energy E of the excited molecule and is independent of previous collisions. Consequently, the energy of the excited molecule undergoes a Markovian process and the probability $p(E,t)$ of finding the molecule at energy E at time t evolves in time according to a master equation of the following form [13]:

$$\begin{aligned} \frac{\partial}{\partial t} p(E,t) = & \int dE' q(E|E') p(E',t) \\ & - \int dE' q(E'|E) p(E,t) \\ & - K(E) p(E,t), \end{aligned} \quad (2.12)$$

where $q(E|E')$ denotes the rate of energy transfer from E' to E . The integral over final energies yields the frequency $\tau^{-1}(E)$ of collisions at the energy E , hence,

$$\tau^{-1}(E) = \int dE' q(E'|E). \quad (2.13)$$

The average waiting time of a molecule with energy E between subsequent collisions is given by the inverse time $\tau(E) = \tau$ which is energy independent. The normalized transition probability is:

$$p(E|E') = \tau q(E|E'). \quad (2.14)$$

The first two terms of the right hand side of Eq. (2.12) describe the impact of collisions, while the third accounts for reactions and possibly also for the radiative decay of the excited molecule. In the next sections, we will show how the Gaussian structure of both the transition probability kernel and the equilibrium distribution of reactants leads to solutions of this master equation. It cannot be overstressed that both of these properties result from the large dimensionality of the reactants and therefore are applicable to polyatomic molecules having a ‘large’ number of degrees of freedom.

3. The collision dynamics

The master equation with a constant mean waiting time τ and the Gaussian transition probability as given by Eqs. (2.6), (2.7) and (2.9):

$$\begin{aligned} p(E|E') = & \frac{\beta}{\sqrt{2\pi(1-(1-\alpha)^2)(N-1)}} \\ & \times \exp \left[- \frac{(E-E' + \alpha(E' - (N-1)/\beta))^2 \beta^2}{2(1-(1-\alpha)^2)(N-1)} \right] \end{aligned} \quad (3.1)$$

can be solved analytically in the absence of the sink-term $-K(E)p(E,t)$. For the sake of convenience we measure energy from the (Gaussian) thermal equilibrium value $(N-1)/\beta$ in units of the standard deviation of the equilibrium fluctuations $\sqrt{N-1}/\beta$, i.e. we introduce

$$x = \frac{\beta}{\sqrt{N-1}} \left(E - \frac{N-1}{\beta} \right) \quad (3.2)$$

as a dimensionless energy.

Using this variable, the collisional part of the master equation is rewritten as

$$\begin{aligned} \frac{\partial}{\partial t} p(x,t) = & \tau^{-1} \int_{-\infty}^{\infty} \frac{dy}{\sqrt{2\pi(1-a^2)}} \\ & \times \exp \left[- \frac{(x-ay)^2}{2(1-a^2)} \right] p(y,t) - \tau^{-1} p(x,t), \end{aligned} \quad (3.3)$$

where $a \equiv 1 - \alpha$. The eigenvalues μ_n and the corresponding eigenfunctions $\psi_n^0(x)$ of the integral operator C defined as

$$Cp(x) \equiv \int \frac{dy}{\sqrt{2\pi(1-a^2)}} \exp\left[-\frac{(x-ay)^2}{2(1-a^2)}\right] p(y) \quad (3.4)$$

fulfilling

$$C\psi_n^0(x) = \mu_n \psi_n^0(x) \quad (3.5)$$

are given by

$$\mu_n = a^n, \quad (3.6)$$

$$\psi_n^0(x) = \phi_n^0(x) \frac{1}{\sqrt{2\pi}} e^{-x^2/2}, \quad (3.7)$$

$$\phi_n^0(x) = \frac{(-1)^n}{\sqrt{n!}} e^{x^2/2} \frac{d^n}{dx^n} e^{-x^2/2}, \quad (3.8)$$

where n is an integer that goes from zero to ∞ . The spectral properties of C as given by Eqs. (3.6), (3.7) and (3.8) may be verified by inspection. The functions $\phi_n^0(x)$ are the Hermite polynomials [17], normalized such that

$$\int_{-\infty}^{\infty} \frac{dx}{\sqrt{2\pi}} \phi_n^0(x)^2 e^{-x^2/2} = 1. \quad (3.9)$$

Note that the functions $\psi_n^0(x)$ and $\phi_n^0(x)$ form a biorthogonal basis set:

$$\int_{-\infty}^{\infty} dx \phi_m^0(x) \psi_n^0(x) = \delta_{n,m}, \quad (3.10)$$

where $\delta_{m,n}$ denotes the Kronecker symbol. The eigenfunctions do not depend either on the collision time τ nor on the relative energy transfer a . The relative energy transfer affects only the eigenvalues and the collision time sets the overall time scale of the problem. The lowest eigenfunction $\phi_0^0(x)$ has the constant value 1 and correspondingly $\psi_0^0(x)$ is a pure Gaussian which coincides with the thermal equilibrium distribution (Eq. (2.4)) in the absence of reaction.

Any initial probability distribution $p_0(x)$ can be expanded in terms of the eigenfunctions $\psi_n^0(x)$

$$p_0(x) = \sum_{n=0}^{\infty} d_n \psi_n^0(x), \quad (3.11)$$

where the coefficients d_n are

$$d_n = \int_{-\infty}^{\infty} dx \phi_n^0(x) p_0(x). \quad (3.12)$$

The normalization of the initial probability distribution $p_0(x)$, implies that $d_0 = 1$.

In the absence of a sink-term the time-evolution of the probability distribution is given by

$$\begin{aligned} p^0(x,t) &= \sum_{n=0}^{\infty} d_n e^{-(1-a^n)t/\tau} \psi_n^0(x) \\ &= p_{\text{eq}}(x) + \sum_{n=1}^{\infty} d_n e^{-(1-a^n)t/\tau} \psi_n^0(x). \end{aligned} \quad (3.13)$$

Since $\int_{-\infty}^{\infty} dx \psi_0^0(x) = 1$ and $\int_{-\infty}^{\infty} dx \psi_n^0(x) = 0$ for $n \neq 0$, the normalization of $p(x,t)$ remains constant for all times. For long times $t \gg \tau/(1-a)$ the probability distribution approaches the stationary distribution $p_{\text{eq}}(x) = \psi_0^0(x) = (1/\sqrt{2\pi}) e^{-x^2/2}$ which in the original energy units coincides with the Gaussian approximation of $p_{\text{eq}}(E)$, see Eq. (2.4). Limiting cases will be treated in the next section.

4. The survival probability

4.1. Formal solution

In presence of a sink-term the number of excited molecules will decrease in time. In the absence of a gas, there may be in the initial state a fraction of molecules that has an energy which is greater than the barrier energy V . Assuming that the radiative rate is negligible, this fraction will necessarily react and one will be left with only those excited molecules whose energy is below the barrier height. In the presence of collisions, the excited molecule will always eventually acquire enough energy to react. These processes are described by the survival probability $S(t)$ which gives the fraction of excited molecules that have not reacted up to time t :

$$S(t) = \int_{-\infty}^{\infty} dx p(x,t). \quad (4.1)$$

The time dependent probability distribution $p(x,t)$ is the solution of the master equation

$$\frac{\partial}{\partial t} p(x,t) = \tau^{-1} \int_{-\infty}^{\infty} dy p(x|y) p(y,t) - [\tau^{-1} + k_{\infty} \kappa(x)] p(x,t), \quad (4.2)$$

where

$$p(x|y) = \frac{1}{\sqrt{2\pi(1-a^2)}} \exp\left[-\frac{(x-ay)^2}{2(1-a^2)}\right] \quad (4.3)$$

denotes the transition probability from the (reduced) energy y to the (reduced) energy x . The normalized unimolecular rate $\kappa(x)$ is defined by Eq. (2.10) and (Eq. (3.2)) to read:

$$\kappa(x) = \left(\frac{x + \sqrt{N-1} - V\beta/\sqrt{N-1}}{x + \sqrt{N-1}} \right)^{N-1} \times \theta \left(x + \sqrt{N-1} - \frac{V\beta}{\sqrt{N-1}} \right). \quad (4.4)$$

It vanishes for reduced energy values smaller than $x_{\min} = \beta V/\sqrt{N-1} - \sqrt{N-1}$ which can take both positive and negative values. If $\beta V > N-1$ the reduced energy at which reaction sets in has a positive value, $x_{\min} > 0$. If this value is sufficiently large, standard rate theory applies, i.e. after a short relaxational period towards a distribution that hardly differs from the equilibrium distribution an exponential decay sets in. The rate is then given by transition state theory, see Eq. (4.18) below.

For large molecules with a high number of degrees of freedom N , x_{\min} may become negative even for rather high barriers. But due to the high power $N-1$ in the unimolecular rate expression as given by Eq. (4.4), the rate of reaction is still extremely small for a large energy range above x_{\min} . Reaction remains a rare event. In this case the regime of nonexponential decay may be rather extended and the final exponential decay rate is not given by transition state theory. It is this large molecule case in which we are mostly interested.

Integrating both sides of the master equation (4.2) over all values of the energy x one obtains the following, seemingly simple equation for the survival probability

$$\dot{S}(t) = -k(t)S(t). \quad (4.5)$$

The time dependent rate $k(t)$ is, however, defined in terms of the solution $p(x,t)$ of the master equation as

$$k(t) = k_{\infty} \frac{\int dx \kappa(x) p(x,t)}{\int dx p(x,t)} \quad (4.6)$$

so that one must solve the master equation to obtain the survival probability. Note that the initial decay rate $k(0)$ is dependent only on the initial distribution of reacting molecules but is *independent* of the collisional dynamics.

The time-dependence of $k(t)$ leads in general to a non-exponential decay that is visible at least at short times. The time-dependence of $p(x,t)$ is determined by the eigenvalues λ_n and the eigenfunctions ψ_n , $n = 0, 1, \dots$, of the ‘master operator’ in the presence of the sink term:

$$\tau^{-1} \int_{-\infty}^{\infty} dy p(x|y) \psi_n(y) - \tau^{-1} \psi_n(x) - k_{\infty} \kappa(x) \psi_n(x) = -\lambda_n \psi_n(x). \quad (4.7)$$

One can show that all eigenvalues λ_n are real, but, in contrast to the problem without a sink, all of them are greater than zero, reflecting the fact that all initially excited molecules will eventually have completely reacted. In the absence of the sink, the lowest eigenvalue is zero and as already mentioned, the distribution evolves to the equilibrium distribution.

The transposed master operator has the same eigenvalues λ_n and corresponding eigenvectors $\phi_n(x)$:

$$\tau^{-1} \int_{-\infty}^{\infty} dy p(y|x) \phi_n(y) - \tau^{-1} \phi_n(x) - k_{\infty} \kappa(x) \phi_n(x) = -\lambda_n \phi_n(x). \quad (4.8)$$

As for the pure collisional dynamics, $\psi_n(x)$ and $\phi_n(x)$ form a biorthogonal set of basis functions, i.e.

$$\int_{-\infty}^{\infty} dx \phi_m(x) \psi_n(x) = \delta_{n,m}. \quad (4.9)$$

Due to detailed balance (Eq. (2.8)) of the collision operator, the eigenfunctions $\psi_n(x)$ and $\phi_n(x)$ are related to each other by

$$\psi_n(x) = \phi_n(x) e^{-x^2/2} / \sqrt{2\pi}. \quad (4.10)$$

Once the eigenvalues and the eigenfunctions are known, the time-dependent solution of the master equation (4.2) reads

$$p(x, t) = \sum_n e^{-\lambda_n t} c_n \psi_n(x), \quad (4.11)$$

where

$$c_n = \int_{-\infty}^{\infty} dx \phi_n(x) p_0(x). \quad (4.12)$$

Here $p_0(x)$ denotes the initial distribution of excited molecules. Integrating over all energies one obtains the survival probability:

$$S(t) = \sum_n e^{-\lambda_n t} c_n q_n, \quad (4.13)$$

where

$$q_n = \int_{-\infty}^{\infty} dx \psi_n(x). \quad (4.14)$$

4.2. Weak absorption limit

If the rate of change of the distribution function is mainly determined by collisions and absorption (reaction) is a rare event, the sink term in the master equation (4.2) can be treated as a small perturbation. The parameter that controls the magnitude of the perturbation is $k_\infty \tau$. The unperturbed solution is given by Eq. (3.13) which when inserted into Eq. (4.6) yields to first order in $k_\infty \tau$ the time dependent weak absorption rate $k_{\text{wa}}(t)$:

$$k_{\text{wa}}(t) = k_\infty \left(k_{00} + \sum_{n=1}^{\infty} k_{0,n} d_n e^{-(1-a^n)t/\tau} \right), \quad (4.15)$$

where d_n are the expansion coefficients of the initial distribution, see Eq. (3.12), and $k_{n,m}$ are matrix elements of the sink-term defined by

$$k_{n,m} = \int_{-\infty}^{\infty} \phi_n^0(x) \kappa(x) \psi_m^0(x). \quad (4.16)$$

The actual strength of the perturbation is also determined by the magnitude of the matrix elements $k_{n,m}$ that approach unity on the diagonal for large n and

are exponentially small in βV for small n . When leaving the diagonal, the absolute value of the matrix-elements rapidly decreases.

When applied to an energy diffusion equation, this approximation was recently shown to give excellent results provided that the reduced barrier energy is larger than unity, $\beta V \gtrsim 3$ [10]. The master equation (4.2) approaches the energy diffusion regime in the limit $\tau \rightarrow 0$, $a \rightarrow 1$ with a small but finite dissipation rate $\gamma = \lim_{\tau \rightarrow 0, a \rightarrow 1} (1-a)/\tau$. Obviously, in this limit the parameter $k_\infty \tau$ is always small. Note that the weak absorption rate (4.15) starts with the correct initial rate $k_{\text{wa}}(0) = k_\infty \sum_{n=0}^{\infty} k_{0,n} d_n = k_\infty \int dx \kappa(x) p_0(x) = k(0)$. One can show that the corresponding survival probability $S_{\text{wa}}(t) = \exp[-\int_0^t ds k_{\text{wa}}(s)]$ always decays faster than the exact one:

$$S_{\text{wa}}(t) \leq S(t). \quad (4.17)$$

For large times, $k_{\text{wa}}(t)$ approaches the value given by transition state theory:

$$\begin{aligned} \lim_{t \rightarrow \infty} k_{\text{wa}}(t) &= k_\infty k_{0,0} = k_\infty \int_{-\infty}^{\infty} dx \kappa(x) \psi_0^0(x) \\ &\equiv k_{\text{TST}}. \end{aligned} \quad (4.18)$$

In Section 5 we will compare this approximation with numerical solutions of the master equation (4.2).

4.3. Strong collision limit

The strong collision limit is obtained if the relative energy transfer parameter $\alpha = 1$ or equivalently $a = 0$. A single collision with a gas molecule suffices to thermalize the reacting molecule. In this limit, the master equation simplifies to:

$$\begin{aligned} \frac{\partial}{\partial t} p(x, t) &= \tau^{-1} p_{\text{eq}}(x) S(t) - \tau^{-1} p(x, t) \\ &\quad - k_\infty \kappa(x) p(x, t). \end{aligned} \quad (4.19)$$

Performing a Laplace transform of this equation one obtains:

$$\hat{p}(x, z) = \frac{p(x, 0) + p_{\text{eq}}(x) \hat{S}(z)}{z + 1 + k_\infty \tau \kappa(x)}, \quad (4.20)$$

where $\hat{p}(x, z)$ is the Laplace transform of the time dependent probability distribution:

$$\hat{p}(x, z) = \tau^{-1} \int_0^{\infty} dt e^{-zt/\tau} p(x, t), \quad (4.21)$$

$\hat{S}(z)$ is the Laplace transform of the survival probability (Eq. (4.1)):

$$\hat{S}(z) = \tau^{-1} \int_0^{\infty} dt e^{-zt/\tau} S(t) \quad (4.22)$$

and $p(x, 0)$ is the initial distribution.

Integrating Eq. (4.20) over the reduced energy one obtains the following exact expression for the Laplace transformed survival probability $\hat{S}(z)$:

$$\hat{S}(z) = \frac{\int dx p(x, 0) / [1 + z + k_{\infty} \tau \kappa(x)]}{1 - \int dx p_{\text{eq}}(x) / [1 + z + k_{\infty} \tau \kappa(x)]}. \quad (4.23)$$

The denominator has an isolated zero that determines the long-time behavior of $\hat{S}(z)$. It coincides with the smallest eigenvalue of Eq. (4.19). The location of this pole is determined by

$$z = k_{\infty} \tau \int dx \frac{\kappa(x) p_{\text{eq}}(x)}{1 + z + k_{\infty} \tau \kappa(x)}. \quad (4.24)$$

This equation is obtained by multiplying the denominator of $\hat{S}(z)$ by $z + 1$ and using the normalization of $p_{\text{eq}}(x)$. It can be solved iteratively. In the rate regime for which $z \ll 1$, the leading approximation to the rate is obtained by putting $z = 0$ on the right hand side of Eq. (4.24). This yields the standard strong coupling expression for the rate [16]:

$$k_{sc} = k_{\infty} \int dx \frac{\kappa(x) p_{\text{eq}}(x)}{1 + k_{\infty} \tau \kappa(x)}. \quad (4.25)$$

For this rate to be small compared to the collision frequency, the overlap of the thermal distribution $p_{\text{eq}}(x)$ and the normalized unimolecular rate $\kappa(x)$ must be small. This implies that the thermal rate must also be small compared to the collision frequency, i.e. $k_{\text{TST}} = k_{\infty} \int dx \kappa(x) p_{\text{eq}}(x) \ll \tau^{-1}$. If this is not the case, Eq. (4.24) must be iterated numerically until convergence is obtained.

When the reaction is also fast i.e. $k_{\infty} \tau \rightarrow \infty$ one finds from Eq. (4.24)

$$k_{\text{scfr}} = \tau^{-1} \int_{x_{\text{min}}}^{\infty} dx p_{\text{eq}}(x). \quad (4.26)$$

This is an exact expression for the least eigenvalue belonging to the master Eq. (4.19) in the limit of infinitely fast reactions. It can be shown that all other eigenvalues are given by the collision frequency τ^{-1} . Consequently, in order to observe an exponential decay with the rate k_{scfr} at finite times, this rate must be small compared to the collision frequency. This will occur only if the reduced barrier height (βV) is much larger than the reduced thermal energy of the reactants (βE_{th}).

4.4. Strong absorption limit

In the strong absorption limit $k_{\infty} \tau$ becomes large. In principle this case can be treated by an expansion in the number of collisions. To find this expansion one rewrites the master equation (4.2) into the following equivalent inhomogeneous integral equation:

$$\begin{aligned} p(x, t) = & \exp\{-[k_{\infty} \kappa(x) + \tau^{-1}]t\} p_0(x) \\ & + \tau^{-1} \int_0^t ds \exp\{-[k_{\infty} \kappa(x) + \tau^{-1}]\} \\ & \times (t-s) \int_{-\infty}^{\infty} dy p(x|y) p(y, s), \end{aligned} \quad (4.27)$$

where $p_0(x) = p(x, 0)$ denotes the initial distribution. Iterating this equation and performing the time integrals one obtains the time-dependent density in terms of the number of collisions:

$$\begin{aligned} p(x, t) = & \exp\{-[k_{\infty} \kappa(x) + \tau^{-1}]t\} p_0(x) \\ & + \sum_{n=1}^{\infty} (k_{\infty} \tau)^{-n} e^{-nt/\tau} \int_{-\infty}^{\infty} dy_1 \dots dy_n \\ & \times \sum_{l=0}^n \frac{\exp[-k_{\infty} \kappa(y_l)t]}{\prod_{m=0, m \neq l}^n [\kappa(y_l) - \kappa(y_m)]} \\ & \times p(x|y_1) \dots p(y_{n-1}|y_n) p_0(y_n), \end{aligned} \quad (4.28)$$

where in the second sum y_0 denotes x . The first term gives the contribution to the density if there is no collision up to time t while the n th term in the sum gives the contribution from n collisions. When $k_{\infty} \tau$ is large, the first term will give the dominant

part of the survival probability. In general, although Eq. (4.28) is an exact representation of the time dependent density, valid for general transition probabilities $p(x|y)$, it is of little practical value since the integrals and sums are difficult to evaluate.

5. Numerical solution of the master equation

To obtain a numerical solution we projected the full eigenvalue problem (Eq. (4.8)) onto the subspace which is spanned by the first M eigenfunctions of the collision operator

$$\phi_n(x) = \sum_{m=0}^{M-1} c_{n,m} \phi_n^0(x) \quad (5.1)$$

and determined numerically the eigenvalues and eigenfunctions of the following approximate algebraic eigenvalue problem

$$\tau^{-1}(a^{n-1} - 1)c_{n,m} + k_\infty \sum_{l=0}^{M-1} k_{m,l} c_{n,l} = \lambda_n c_{n,m}. \quad (5.2)$$

The matrix elements $k_{m,l}$ of the sink term are defined by Eq. (4.16). For the range of parameters considered in this paper, this approximation gives stable numerical results for at least the first 10 low-lying eigenvalues and eigenfunctions when using a basis set with $M = 30$ functions. For larger values of βV than used below, or values of a closer to one than those considered here, a larger basis set would be required.

5.1. Eigenvalues

When the gap between the two lowest eigenvalues is large, one will find a short transient time followed by single exponential decay, with a rate given by the lowest eigenvalue. Nonexponential decay will be observed if the gap between these two eigenvalues is small. Fig. 2 shows the ratio of the first two eigenvalues λ_0 and λ_1 as a function of the fraction of energy transferred per collision $a = 1 - \alpha$ (cf. Eq. (2.5)) for different values of $k_\infty \tau$ and βV . For most parameter values there is a pronounced gap between the first and the second eigenvalue. The gap increases with decreasing $k_\infty \tau$. Note that $\tau \rightarrow 0$ leads

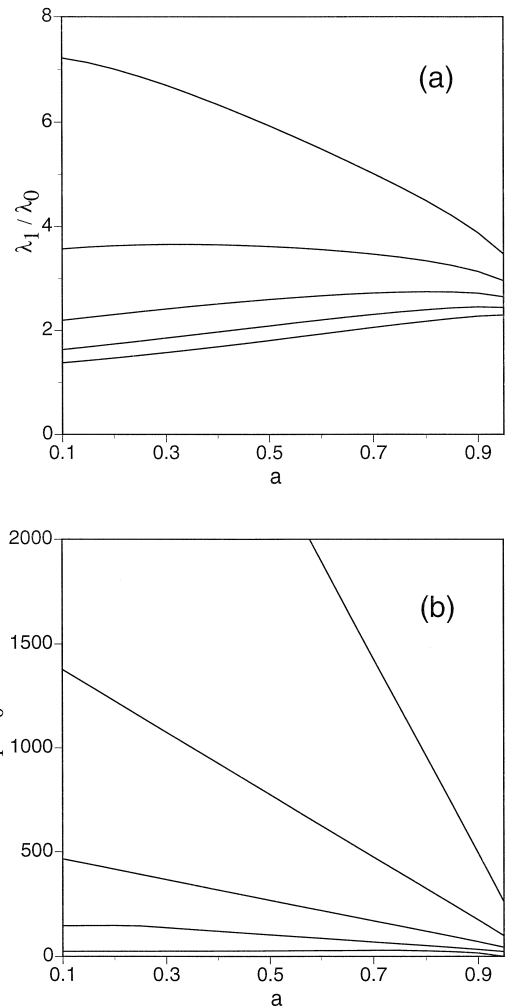


Fig. 2. Ratio of the smallest eigenvalues λ_1/λ_0 plotted as a function of the relative average transferred energy. Panels (a) and (b) correspond to high ($\beta V = 5.77$) and low ($\beta V = 11.55$) temperature respectively. The solid lines, from top to bottom correspond to the values of $k_\infty \tau = 10^2, 10^{2.5}, 10^3, 10^{3.5}, 10^4$, respectively.

to the high pressure limit, where one expects single exponential decay. For large values of $k_\infty \tau$ the ratio λ_1/λ_0 is an increasing function of the parameter a . However, for smaller values the ratio turns into a decreasing function of a . Since the matrix-elements $k_{n,m}$ decrease exponentially with increasing barrier height βV , the gap between the first and second eigenvalue rapidly increases with βV as may be seen by comparison of panels (a) and (b) of the figure.

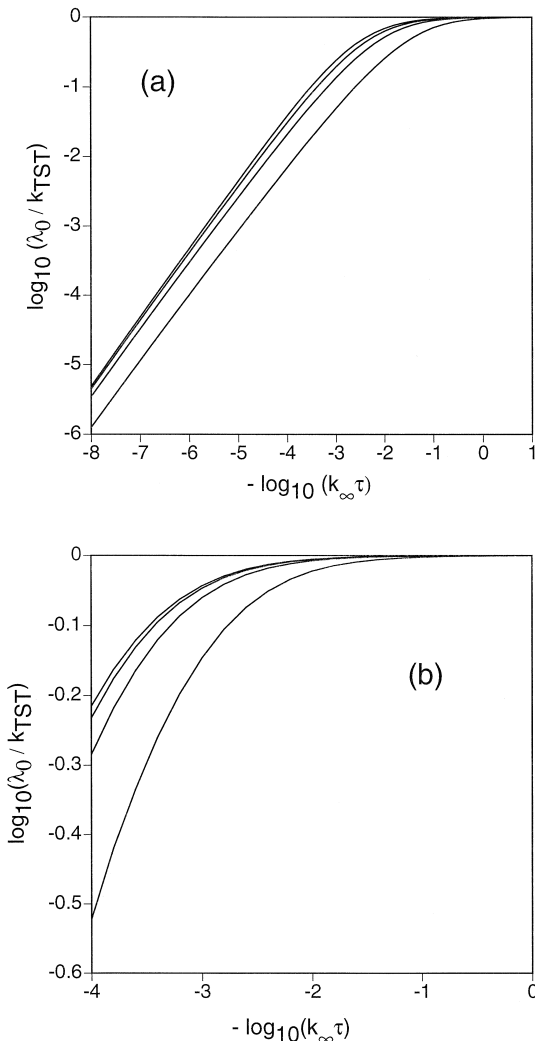


Fig. 3. Pressure $(\tau)^{-1}$ and prefactor k_∞ dependence of the smallest eigenvalue. The transition state theory rate is defined in Eq. (4.18). The solid lines from bottom to top correspond to increasing values of the relative energy transferred per collision, $a = 0.9, 0.6, 0.3, 0.001$, respectively. Panel (a) is for $\beta V = 5.77$ while panel (b) is for $\beta V = 11.55$.

For large values of $k_\infty \tau$ the smallest eigenvalue λ_0 apparently goes to zero as $(\tau)^{-1}$ as can be seen from the slope of the lines in Fig. 3. This asymptotic behaviour may be understood from the following argument: If reaction is very fast, each excursion of the energy of the excited molecule above the barrier energy will almost surely lead to reaction. Hence one can regard all states with energies larger than the

barrier energy as totally absorbing. In this limit, the master equation (4.2) becomes:

$$\begin{aligned} \frac{\partial}{\partial t} p(x, t) &= \tau^{-1} \int_{-\infty}^{x_{\min}} dy p(x|y) p(y, t) \\ &\quad - \tau^{-1} p(x, t). \end{aligned} \quad (5.3)$$

The upper limit of the integral on the right hand side is the dimensionless barrier height $x_{\min} = \beta[V - (N - 1)/\beta]/\sqrt{N - 1}$. For larger values of x absorption causes the probability to vanish. Accordingly, the eigenvalue problem becomes

$$\begin{aligned} \tau^{-1} \int_{-\infty}^{x_{\min}} dy p(x|y) \tau^{-1} \psi_n(y) - \psi_n(x) \\ = -\lambda_n \tau \psi_n(x). \end{aligned} \quad (5.4)$$

Since the transition probability $p(x|y)$ is independent of the collision time in this fast reaction limit, all eigenvalues are proportional to the collision frequency τ^{-1} . Of course, the lower the temperature, the larger must the prefactor be in order to reach this limit, this is clearly seen by comparing panels (a) and (b) of the figure.

For $k_\infty \tau$ of the order of one, the rate approaches the transition state theory (TST) value. For smaller values of a , i.e. for a larger average energy transfer per collision the crossover region shifts to larger values of $k_\infty \tau$. For larger barriers βV , the TST rate limit is approached at larger values of $k_\infty \tau$.

5.2. Decay of the distribution

The time dependent distribution $p(x, t)$ is determined from the eigenvalues and eigenfunctions obtained from diagonalization of Eq. (5.2). Given the eigenfunctions, one determines the coefficients c_n from Eq. (4.12). To obtain the time dependent distribution one must first define the initial one. In this subsection the initial distribution is chosen as a Gaussian

$$\begin{aligned} p_0(x, t) &= \sqrt{s/(2\pi)} \\ &\quad \times \exp\left\{-s^2 \left[x + (1 - 1/s)\sqrt{N - 1} \right]^2 / 2\right\}, \end{aligned} \quad (5.5)$$

which approximately describes a Boltzmann distribution of energy at an inverse temperature $s\beta$. For

$s = 1$ the vibrational states of the excited molecule are in thermal equilibrium with the surrounding gas while the molecule is cooler (hotter) than the gas for $s > 1$ ($s < 1$). The time-dependent distribution $p(x,t)$ is then determined from Eq. (4.11). If the initial temperature s is not too far from unity, and if the collisions are not too weak, i.e. $k_\infty\tau$ is not too large, only the first few coefficients c_n contribute substantially to the sum (Eq. (4.11)) representing the time-dependent distribution of energy. One can therefore

truncate the sum at a convenient level. In our computations, we chose 30 basis functions.

The evolution of the time dependent distribution is shown in Fig. 4. Panel (a) corresponds to $s = 1.2$, i.e. an initial temperature which is lower than the temperature of the gas which is taken as $\beta V = 5.77$. As time increases, the population is depleted and the amplitude of the distribution $p(x,t)$ decreases. It approaches the form of the lowest eigenfunction $\psi_0(x)$, as shown in the inset. Note that the lowest

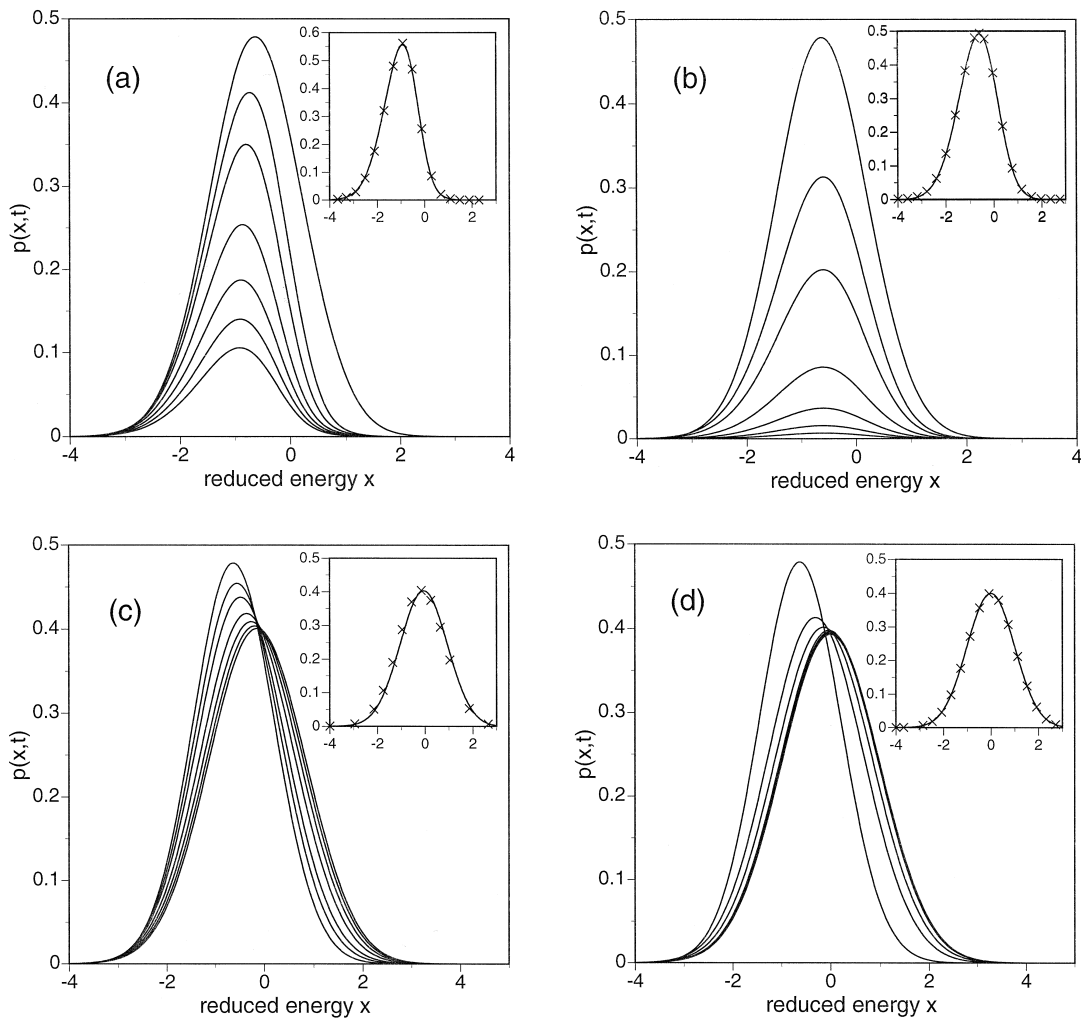


Fig. 4. Time and energy dependence of the distribution function $p(x,t)$. The solid lines (from top to bottom) correspond to the reduced times of $k_\infty t = 0, 1000, 2000, 4000, 6000, 8000, 10000$. The initial distribution is Gaussian (cf. Eq. (5.5)) with a temperature which is lower than the gas temperature ($s = 1.2$). The relative energy transfer is moderate, $a = 0.85$. Panel (a) corresponds to $\beta V = 5.77$, $k_\infty\tau = 10^3$, panel (b) is for $\beta V = 5.77$, $k_\infty\tau = 2 \times 10^2$, panel (c) is for $\beta V = 11.55$, $k_\infty\tau = 10^3$ and panel (d) is for $\beta V = 11.55$, $k_\infty\tau = 2 \times 10^2$. The inserts show the respective eigenfunctions $\psi_0(x)$ (full line) and distributions (crosses) renormalized to unit area at $t = 10000$.

eigenfunction differs substantially from the equilibrium distribution, which would be a Gaussian centered at $x = 0$. The long collision time causes the high energy fraction to decay faster than the low energy fraction so that at long times, one remains with most of the population substantially below the average thermal energy. Increasing the pressure, or equivalently, increasing the prefactor k_∞ causes a faster depletion of the reactants, as may be seen by comparing panel (b) with panel (a). The only difference between the two panels is that $k_\infty\tau$ is 5 times larger in panel (a).

Increasing the barrier height, which corresponds to lowering the temperature of the gas, causes a dramatic change. Panel (c) shows the evolution of the distribution for $\beta V \approx 12$ and should be compared to panel (a). Due to the high barrier, almost no decay takes place. Due to the large gap between the lowest and the first eigenvalue, the distribution function tends to the lowest eigenfunction before any substantial decay sets in. This eigenfunction is almost identical to the equilibrium distribution as may be noted from the symmetry about $x = 0$. These results are insensitive to the pressure or the magnitude of the prefactor, as evidenced from panel (d) which is at the same low temperature as panel (c), but at the high pressure of panel (b).

5.3. Decay of the survival probability

The survival probability is obtained from Eq. (4.1) using the numerically computed time dependent probability distribution $p(x,t)$, or, equivalently from Eq. (4.13). We computed the sum (4.13) truncated after 30 terms. Results are shown in Fig. 5. The structure of the logarithmic plots of the survival probabilities is governed by the initial rate k_0 which determines the initial slope, and the smallest eigenvalue λ_0 which determines the asymptotic slope at large times. The time scale of change from the initial

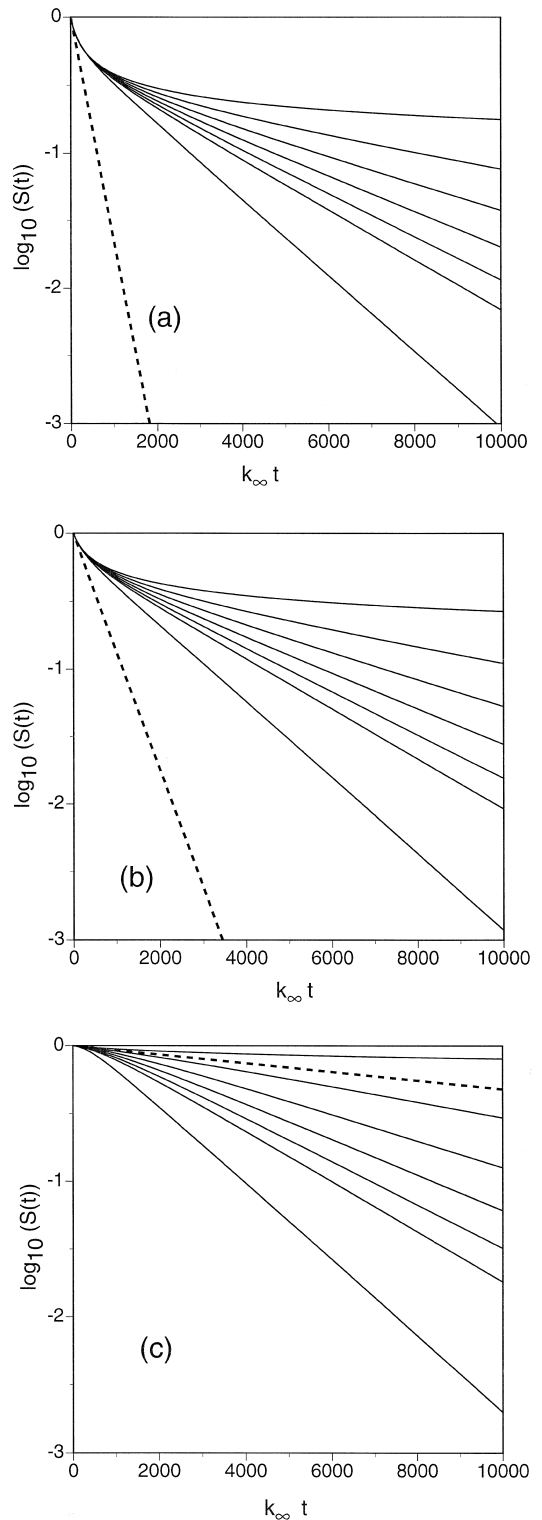


Fig. 5. Time dependence of the logarithm of the survival probability $\log_{10}(S(t))$. The initial distribution is Gaussian (cf. Eq. (5.5)). The solid lines from top to bottom correspond to $(k_\infty\tau)^{-1} = 0, 10^{-3}, 2 \times 10^{-3}, 3 \times 10^{-3}, 4 \times 10^{-3}, 5 \times 10^{-3}, 10^{-2}$. Panel (a) is for $\beta V = 5.77$, $s = 0.9$ and $a = 0.9$; panel (b) is for $\beta V = 5.77$, $s = 1$, and $a = 0.85$; and panel (c) is for $\beta V = 5.77$, $s = 1.5$ and $a = 0.85$. The dashed line corresponds to the initial (TST) decay rate.

to the final slopes is determined by the magnitude of the next smallest eigenvalues and hence is of the order of λ_1^{-1} .

Since the initial rate is independent of the dynamics of the collisions, survival probabilities with different pressure, start out at $t = 0$ with the same slope and only then change to a different behavior. The smaller τ , i.e. the higher the pressure and the shorter is the time between collisions, the faster the final exponential decay is approached.

Panel (a) shows the decay for an initial temperature ($s = 0.9$) which is greater than the gas temperature. The solid lines from top to bottom correspond to increasing pressure, or equivalently increasing values of $(k_\infty\tau)^{-1}$. The dashed line shows the TST rate (cf. Eq. (4.18)) at the initial temperature ($s = 0.9$). For short times the decay at all pressures is fast and approximately equal to the TST rate at $s = 0.9$. As time increases, the high energy part of the initial population is depleted and the rate slows down. In the absence of collisions, the survival probability reaches a plateau value, reflecting the population of reactants whose energy is below the barrier height and thus cannot react. Collisions with a buffer gas, will ultimately raise the energy of these remaining reactants above the barrier and they will react. Increasing the pressure will thus increase the decay rate at long times. The magnitude of the long time decay rate will reflect the pressure. At high enough pressure, this rate will approach the thermal TST rate but at the temperature of the gas ($s = 1$), which in the case shown in panel (a), is lower than the initial temperature.

Panel (b) shows the pressure dependence of the decay rate when the initial distribution is at the same temperature as the gas ($s = 1$). The dashed line is the initial thermal TST decay rate. In this case, the high pressure decay rate is approximately equal to the initial decay rate at all times. This is the ‘standard’ case, in which the initial decay rate at all pressures is indeed approximately equal to the thermal rate. At long times and low pressure there is a slowing down of the rate, increasing the pressure brings one back to the upper limit TST rate.

Lowering the initial temperature below the gas temperature as shown in panel (c) ($s = 1.5$), causes a qualitative change. The initial thermal TST rate (dashed line) is slower than the long time rate in the

presence of collisions. Adding a buffer gas at room temperature heats up the molecule and at high pressure one approaches the room temperature decay rate which is much higher than the initial rate. This is the scenario observed in the experiment of Balk and Fleming, which will be analysed in more detail in the next subsection.

5.4. Application to the isomerization of *trans*-stilbene

As noted in the Introduction, the central purpose of studying the binary collision theory was to understand the observed fluorescence decay plots of *trans*-stilbene. To apply the theory one must first set the correct physical parameter range. The isomerization rate in atmospheric pressure liquid at room temperature is approximately $(30 \text{ ps})^{-1}$ [7]. The activation energy in the liquid is also known (~ 3.4 kcal/mole), so that at $T = 300 \text{ K}$ $V/k_B T = 5.77$. This sets the prefactor and one finds $k_\infty^{-1} = 9.4 \times 10^{-14} \text{ s}$.

To obtain the initial low temperature of the theoretical distribution, we fit the initial slope of the isolated molecule decay to the experimental initial slope. This leads to an initial temperature of 230 K.

The mean collision time may be estimated from gas kinetic theory [18] as

$$\tau = \frac{\sqrt{mk_B T}}{P\pi r^2} \quad (5.6)$$

where m is the mass of the gas molecule (for methane $m = 16$ a.m.u.), P is the pressure and $r = 4.1 \text{ \AA}$ is the sum of approximate hard sphere radii of the stilbene and methane molecules (1.1 \AA for methane and 3.0 \AA for *trans*-stilbene). At a pressure of 1 atm and $T = 300 \text{ K}$, one finds that $\tau \approx 115 \text{ ps}$. At room temperature this means that $k_\infty\tau \approx 1220$. Finally the radiative lifetime of *trans*-stilbene in the S_1 state as given in Ref. [1] is $3.75 \times 10^8 \text{ s}^{-1}$.

Thus far all parameters are set by experiment. To complete the model we need two additional parameters. One is the effective number of degrees of freedom (N) of the stilbene molecule, to be used in the RRK expression for the rate. We set this number at 15, guided by the number of low frequency modes found in the potential energy surface of Vachev et al

[19], as described in Ref. [5]. The remaining parameter is the relative energy transferred per collision α , cf. Eq. (2.7). This parameter was optimized to $\alpha = 0.8$, to obtain a reasonable fit with the experimental decay curves. This number is quite reasonable when compared with experimental results for other polyatomic molecules [12].

A comparison between the experimental decay curves and the results of our model, including the radiative decay (which was ignored in Fig. 5), is shown in Fig. 6. The solid lines from top to bottom correspond to varying the pressure from 0 to 5 atm. with an increment of 1 atm. The theoretical decay rates (solid lines), are compared with the experimental rates, shown as dotted lines in the figure. We believe that the agreement between experiment and theory as shown in Fig. 6 is satisfactory. The pressure dependence of the survival probability is reasonably well accounted for by the theory. The dashed line shows the decay based on the initial rate. This initial rate is faster than the rate in the absence of collisions but slower than the decay at higher buffer gas pressure. It is this seemingly strange behavior which puzzled Balk and Fleming. Here we see that the present model, based on an initial low temperature of the reactants fully explains this result.

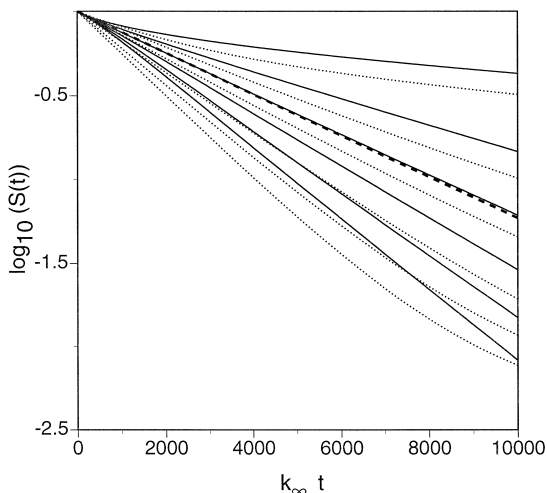


Fig. 6. Comparison of the theoretical and experimental time and pressure dependence of the survival probability. The solid lines from top to bottom correspond to the theoretical prediction for pressures varying from 0 atm to 5 atm of methane gas. The dotted lines show the experimental measurements. The dashed line shows the decay with the initial rate. For further details, see the text.

The most notable difference between experiment and theory as presented in Fig. 6 is the faster decay measured experimentally. This difference probably results from our very crude approximation for the initial distribution. We have assumed that it may be approximated in terms of a single temperature. In fact, Balk and Fleming resort to three different ‘temperatures’ to describe the decay in the absence of collisions, suggesting that the laser excitation gives a rather complicated initial distribution. Adding an initial component at temperatures higher than 230 K to our theoretical analysis will change the shape of the isolated molecule decay curve, the fast component would lead to a lower survival probability. However this would be a purely empirical exercise, we preferred to provide the bare results obtained without any further tailoring of parameters.

6. Discussion

A binary collision theory for polyatomic molecules has been presented. In contrast to Kramers’ one dimensional theory, when dealing with polyatomic molecules, the decay rate can be sensitive to the initial conditions, provided that the number of active degrees of freedom of the polyatomic molecule (N) is larger than the reduced barrier height ($V/k_B T$). In this limit, the average energy of reactants is greater than the barrier height, and even the isolated molecule will undergo reaction. Collisions will enhance the rate further by providing energy to reactants whose initial energy is too low.

This dependence on the initial conditions will cause a qualitative change in the pressure dependence of the survival probability. If the initial temperature is lower than the gas temperature, the initial decay rate will be lower than the high pressure TST limiting rate. If the initial temperature is greater than the gas temperature then the initial rate will be larger than the high pressure limiting TST rate. The stilbene isomerization belongs to the former class, a reasonable estimate for the initial temperature of trans-stilbene is 230 K, in good qualitative agreement with predictions based on molecular dynamics computations [5,6].

The model presented in this paper is quite crude. We have used RRK densities of states and cross sections. This is not really necessary. The important condition would be that the exact quantum thermal density of states resembles a Gaussian. Given the quantum density of states, one could map it onto a Gaussian form at any given temperature and if the Gaussian approximation is reasonable then the present formalism is applicable. Moreover, one does not need to use the RRK expression for the energy dependent cross section one could use better theoretical or experimental determinations of the energy dependent reaction rate.

The most restrictive assumption in the present theory is the use of a Gaussian transition probability kernel for the energy relaxation. Fortunately, the study of energy relaxation of a series of polyatomic molecules [11,12] shows that this is actually not too bad an approximation as long as the initial energy does not deviate too strongly from the thermal energy at the gas temperature. In fact, one would suspect that in most cases in which the reactants are prepared by laser excitation from a room temperature S_0 state to an S_1 state, such that the laser frequency corresponds to ω_{00} , the temperature in the excited state would not deviate too far from room temperature and the present theory would be applicable.

An independent experimental verification of the cooling mechanism of the trans-stilbene isomerization would be obtained by time resolved monitoring of the emission spectrum of the reactants. If the reactants are initially cold and are subsequently heated by collisions with a gas, one should see a time dependent shift of the emission spectrum from the red to the blue. The present binary collision theory would be well suited to analyze such an experiment, since it readily provides the time resolved energy population of the reacting species.

Acknowledgements

AMB thanks the Hebrew University for his appointment as a Forchheimer Professor at the Institute

of Chemistry. EP and PT acknowledge the hospitality of Prof. P. Hänggi and his group in Augsburg, where part of this work was carried out. EP also thanks the Humboldt Foundation for a senior Humboldt award which enabled part of this research. This work was also supported by grants from the Minerva Foundation, Munich/Germany, the German Israeli Foundation for Scientific Research and Development, the U.S. – Israel Binational Science Foundation and the Russian Foundation of Fundamental Research (Grant No. 95-03-09133a).

References

- [1] M.W. Balk, G.R. Fleming, *J. Phys. Chem.* 90 (1986) 3975.
- [2] K.F. Freed, D.F. Heller, *J. Chem. Phys.* 61 (1974) 3942.
- [3] E.W. Montroll, K.E. Shuler, *J. Chem. Phys.* 26 (1957) 454.
- [4] E.W. Montroll, K.E. Shuler, *Adv. Chem. Phys.* 1 (1958) 361.
- [5] G. Gershinsky, E. Pollak, *J. Chem. Phys.* 107 (1997) 812.
- [6] G. Gershinsky, E. Pollak, *J. Chem. Phys.* 107 (1997) 10532.
- [7] J. Schroeder, D. Schwarzer, J. Troe, F. Voß, *J. Chem. Phys.* 93 (1990) 2393.
- [8] H.A. Kramers, *Physica* 7 (1940) 284.
- [9] V.I. Mel'nikov, S.V. Meshkov, *J. Chem. Phys.* 85 (1986) 1018.
- [10] E. Pollak, P. Talkner, A.M. Berezhkovskii, *J. Chem. Phys.* 107 (1997) 3542.
- [11] I. Oref, B.C. Tardy, *Chem. Rev.* 90 (1990) 1407.
- [12] U. Hold, T. Lenzer, K. Luther, K. Reihls, A. Symonds, *Ber. Bunsenges. Phys. Chem.* 101 (1997) 552.
- [13] W. Forst, *Theory of unimolecular reactions*, Academic Press, New York 1973.
- [14] N.B. Slater, *The theory of unimolecular reactions*, Cornell University Press, Ithaca, New York, 1959.
- [15] N.G. van Kampen, *Stochastic processes in physics and chemistry*, North Holland, Amsterdam, 1992.
- [16] P. Hänggi, P. Talkner, M. Borkovec, *Rev. Mod. Phys.* 62 (1990) 251.
- [17] M. Abramowitz, I.A. Stegun, *Handbook of mathematical functions*, Dover Publications, New York, 1965.
- [18] W.J. Moore, *Physical Chemistry*, Prentice-Hall, N.J., 1962, p. 274 ff.
- [19] V.D. Vachev, J.H. Frederick, B.A. Grishanin, V.N. Zadkov, N.I. Koroteev, *J. Phys. Chem.* 99 (1995) 5247.